UNIVERSITY of CALIFORNIA

SANTA CRUZ

THE QUANTUM HALL EFFECT AS A TOPLOGICAL STATE

A thesis submitted in partial satisfaction of the

requirements for the degree of

BACHELOR OF SCIENCE

in

APPLIED PHYSICS

by

Zachary A. Kober

17 August 2018

The thesis of Zachary A. Kober is approved by:

Professor Arthur P. Ramirez
Thesis Advisor

Professor David M. Smith
Thesis Coordinator

Professor Robert P. Johnson
Chair, Department of Physics

Contents:

1 Introduction

Quantum Hall physics is the study of the nature of the electron when confined to a two-dimensional material under the presence of a strong, perpendicular magnetic field. Under such conditions, electrons will exhibit something called the quantum Hall effect which can be most noticeably described as the quantization of the Hall conductivity.

$$\sigma_H = \frac{e^2}{2\pi\hbar}\eta \qquad (1)$$

This is shown by Equation (1) where σ_H is the Hall conductance, e is the electric charge, ħ is a reduced Planck's constant $\hbar = \frac{h}{2\pi}$, and η is the quantum number associated with the various quantum states of the Hall conductance [1].

In Equation (1) the value of η reveals which type of quantum Hall effect is being demonstrated. Experimentally, this number was first seen to take on only integer values, in which the Hall conductivity existed in clearly defined plateau steps and could be described by what is referred to as the integer Hall effect [2]. It wasn't until 1983 that the quantum number η was experimentally validated for an additional fractional set of discrete values where, due to higher quality samples, the Hall conductance was seen to exist in smaller, less clearly defined steps along with the previously demonstrated integer values. This effect is commonly referred to as the fractional quantum Hall effect [3][4]. The delineation between these two effects, besides the integer or fractional value of η, can be attributed to the fact that the resolution of the quantum Hall effect is directly connected to the quality of the sample [5].

These discoveries, explored more fully in Section 2, play a very important role in our understanding of electron-electron interactions in two dimensions as they introduced the idea of topological quantum states of condensed matter in electron systems [6]. The impact of topology within the field of condensed matter physics can be illustrated by pointing out some key characteristic of this effect. This paper, in addition to presenting the basic ideas on which the theory for the quantum Hall effects rests, serves to demonstrate the effects overall topological nature through a specific exploration of the integer quantum Hall effect.

1.1 The Classical Hall Effect

In order to understand the relationship between the quantum Hall effect and topological states of condensed matter it is important to first gain an understanding of the classical Hall effect. Discovered by Edwin Hall in 1879, this effect describes the motion of a charged particle within a magnetic field. The classical Hall effect can be easily demonstrated by driving a current through a sample in the presence of a perpendicular magnetic field [7]. Referencing Figure (1) below, the magnetic field, B (in the z-direction) will cause the electrons within the sample to bend in a counterclockwise circle. With an induced current, I_x, sent through the sample, electrons will accelerate until their motion is balanced by loss through scattering. The charge carriers, in the presence of the magnetic field, will experience a Lorentz force deflecting them towards one side of the sample creating an electric field in the y-direction such that in a steady-state this field will be strong enough to exactly cancel out the magnetic force and the electrons will be pushed straight through the sample (in the x-direction). It is this induced electric field that is responsible for the Hall voltage, V_H, which describes a potential perpendicular to both the current and to the applied magnetic field [8][9].

It is important to note that in this picture, the Drude model, detailed below, is used to provide a simple explanation of charge transport where the electrostatic potential between electrons is ignored and each particle is treated classically. In this model electrons will be seen to bounce and off heavier, relatively immobile positive ions neglecting any long-range interaction between the ions or between the electrons. Additionally, after a collision, the velocity and direction of an electron will be independent of the velocity of the electron before the collision allowing for the force accelerating the electrons to be balanced by scattering [10].

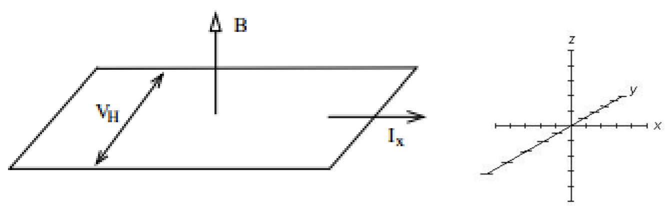

Figure 1: Classical Hall effect diagram [11].

1.1.1 <u>Drude Model</u>

Using the Drude model to describe this system, it is possible to theoretically predict the longitudinal resistance, along the direction of the current, and the transverse resistance (Hall resistance) in the direction of the Hall potential. The derivation in this section is adapted from three reviews [9][11][12]. Applying Newton's second law along with the Lorentz force, an equation of motion can be obtained for the particles described above.

$$m\frac{dv}{dt} = - eE - ev \times B - m\frac{v}{\tau} \tag{2}$$

In Equation (2), v represents the velocity, E is the electric field, B the magnetic field, m is the mass, e is the electric charge, and τ is the material specific scattering time. This scattering time, τ, is an important component to include in this model as it is the time between collisions within the sample as electrons scatter off of impurities, lattice vibrations, magnetic fluctuations or even other electrons.

Setting $\frac{dv}{dt}$ = 0, which describes the system at equilibrium, this can be re-arranged into the format seen in Equations (3) below.

$$-\frac{e\tau}{m}E = v + \frac{e\tau}{m} v \times B; \quad (3)$$

Making use of a fairly simple definition for the current density:

$$J = -nev \quad (4)$$

Where in Equation (4) J is the current density and n is the number of electrons in the system, this can be further simplified into a matrix form shown by Equation (5),

$$\begin{pmatrix} 1 & \frac{eB\tau}{m} \\ \frac{-eB\tau}{m} & 1 \end{pmatrix} J = \frac{e^2 n\tau}{m} E \quad (5)$$

Or more conveniently written in terms of the conductivity, σ, as in Equation (6).

$$J = \sigma E; \qquad \sigma = \frac{n\tau e^2}{m(1+(e\tau b/m)^2)} \begin{pmatrix} 1 & \frac{eB\tau}{m} \\ \frac{-eB\tau}{m} & 1 \end{pmatrix} \quad (6)$$

Here, as the resistivity, ρ, is inversely proportional to the conductivity, ρ = σ^{-1}, it follows that the transverse resistance, will correspond to σ_{xy}, and the longitudinal resistance will correspond to σ_{xx}. This can be seen by referencing a more generalized version of Equation (5) using the conductivity tensor shown in Equation (7) below with x and y representing directional components.

$$\sigma = \begin{pmatrix} \sigma xx & \sigma xy \\ -\sigma xy & \sigma xx \end{pmatrix} \tag{7}$$

For the case of the transverse resistance, the resistivity, which usually different by some geometric factor, will instead coincide nicely without having to divide by any dimensional components of the sample. This can be seen by referring back to Figure (1) where the voltage, $V_{H,}$ is in the y-direction and the resulting current, I_x, is in the x-direction. Using Ohms law, it is not hard to see that the transverse resistance will be proportionate to the resistivity, $\rho_{xy,}$ such that $R_H = -\rho_{xy.}$ The longitudinal resistance can be found by once again referencing the conductivity tensor and dividing by the appropriate sample lengths to extract the resistivity such that $R_{xx} = L/W\rho_{xx.}$ These resistive relationships for the longitudinal and transverse or Hall resistance, stated without further derivation, are shown in Equations (8) and (9) below [9][11][12].

$$R_H = \frac{B}{ne} \tag{8}$$

$$R_x = \frac{L/W}{ne\tau} \tag{9}$$

In Equation (8) R_H is the Hall coefficient and ne is the charge density of the sample. Equation (9) describes the longitudinal resistance, R_x, where L is the length of the sample and W is the width.

These two equations are crucial to understanding the classical Hall effect as they demonstrate a unique geometric property. The Hall resistance is seen to have a linear dependence on the applied magnetic field where as the longitudinal resistance has no dependence on the magnetic field at all. This idea is further supported by looking at the graphical interpretation of the Drude model for both of the resistances as shown in Figure (2) below.

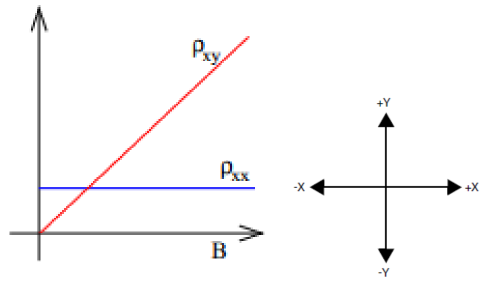

Figure 2: Drude model Graphs. Pxy is the Hall resistance, Pxx is the longitudinal resistance [11].

Considering the independence of the transverse resistance on the sample geometry, Equation (8), if the sample were to be suddenly filled with holes, effectively reducing the area, the longitudinal resistance would change dramatically but Hall resistance would remain the same. If these holes are thought of as impurities within the sample, as each hole can be said to represent a potential barrier that the electrons are forced to interact with, it is clear that in the presence of such impurities the invariant relationship between the sample geometry and the Hall resistance would still exist. The difference between the longitudinal and transverse resistances is meaningful because it suggests that if a topological state were to exist the Hall effect would be a good test as it has a clear dimension dependent feature [13].

1.2 Topology and Quantum Mechanics

In order to explore this more detailed, quantum mechanical description of the underlying physics that govern the quantum Hall effect it is necessary to first understand how topology, a central theme of this paper, relates to quantum mechanics. This can be most noticeably done by examining the experimental evidence presented with the discovery of the integer Hall effect as show in Figure (3) below.

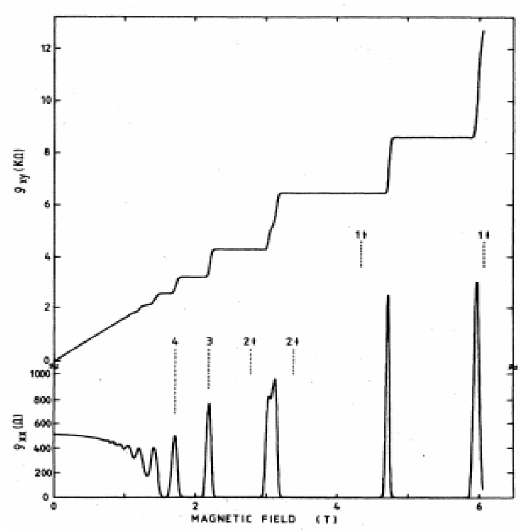

Figure 3: The top curve is the hall resistance; the bottom curve is the longitudinal resistivity. This plot reflects the resistivity and resistance of a heterostructure as a function of the magnetic field at a temperature of approximately 8mK and a fixed carrier density [12].

The integer Hall effect, first experimentally performed by von Klitzing in 1980, demonstrates the expected resistive values, shown in Equation (1), with each transition occurring at integer values of η [2]. This figure is relevant to our current discussion because it shows drastically different attributes to those predicted in Figure (2) which relied on the Drude model. As we will later see in Section 2 of this paper, the Hall resistance existing in number of flat plateau steps instead of a linear slope can be explained topologically as every plateau can be viewed as a different type of topological state entered by virtue of a new ratio of magnetic field to carrier density.

However, before this concept can be elucidated it is useful to understand what topology is on a more fundamental level. Originally, topology was (and still is) a branch of mathematics used to describe three dimensional materials by classifying them as topologically trivial or nontrivial surfaces. This classification sets topologically trivial surfaces as those containing no holes like a ball or a cup (without a handle) and topologically nontrivial surfaces as those which contain at least one hole, like a donut. Additionally, it introduces the idea of topological equivalence, which states that like surfaces can be smoothly transformed into one another [14]. As applied to condensed matter physics, topological classes of matter are generally defined by whole number integers which cannot change continuously and take trivial values such as zero or one in regular matter [15].

For these definitions to apply to quantum mechanics, theoretical physicists were forced to greatly generalize the logic behind topology and apply these ideas to a system in a state of quantum entanglement in which the quantum states of two or more objects could be described with reference to one another. Topology in this respect distinguishes between the two cases describing the topologically trivial case as being when each part of a system is seen as an independent state and where a measurement on one part will have no effect on other parts of the system. In contrast, the topologically nontrivial state in defined such that a measurement on one part of the system will have an impact on the other parts of the system (which are no longer seen as independent). As in the mathematical definition for topology, the idea of topological equivalence in which like trivial or non-trivial states can be smoothly transformed into one another still applies.

At the time of its discovery, the quantum Hall effect had a significant impact within the field of condensed matter physics because it was the first experimental verification of such a nontrivial state in electron systems [6]. Additionally, this effect was especially useful as it demonstrated several topological properties unique to quantum states of matter. Unlike the standard definition of topology, topological states of quantum matter, due to the nature of quantum entanglement, experience some unusual characteristics near the edges of a material where the entanglement stops [9][11]. Furthermore, as topologically defined states (whole number integers) cannot change continuously, the quantum Hall effect helps to demonstrate that it is not possible to go from having topologically non-trivial to trivial properties until a certain threshold is met [6]. This was demonstrated by looking at the flat plateau values of Figure (3). A more detailed description of topological states as applied to the quantum Hall effect as well as the physics describing the edge modes of a sample will be investigated more comprehensively in Section 2.

1.3 Landau Quantization

Before demonstrating the topological nature of the quantum Hall effect, it is necessary to first describe the underlying physics of an electron experiencing this effect from a quantum mechanical perspective. The quantized conductivity of the Hall effect, demonstrated in Equation (1) and observationally explained in Figure (3), clearly suggests that a more inclusive model than the one provided in Section 1.1.1 must be adapted to achieve this goal. This model can be accurately built by a process called Landau quantization in which we find a Hamiltonian to describe the particles within the sample and then use that to solve for a spectrum of allowed eigenfunctions [16]. It is important to note that this derivation, while used to describe the quantum Hall effect, applies to any single, free electron in the presence of a magnetic field.

The Lagrangian for the experimental set up described in Section 1.1 moving through the magnetic field B = ∇ x A is shown in Equation (10) below:

$$L = \frac{1}{2} m\dot{r}^2 - e\dot{r} \cdot A \qquad (10)$$

Here m is the mass of a single particle, A is the magnetic vector potential and r, the position of the electron, can be defined as r = (x, y) as the particle is confined to a two-dimensional plane. Knowing that the Hamiltonian is related to the Lagrangian by equation (11),

$$H = \sum \dot{r}\, p - L \qquad (11)$$

where H is the Hamiltonian and $p = \frac{\partial L}{\partial \dot{r}} = m\,\dot{r} - eA$ is the canonical momentum, we arrive at a Hamiltonian which describes the energy of a particle with a mechanical momentum

μ = p + eA, shown by Equation (12) [16][17].

$$H = \frac{1}{2m} (p + eA)^2 \qquad (12)$$

As the Hamiltonian can be denoted to refer to either the x or y direction it is convenient to index this momentum, μ, as in Equation (13), where subscript i is made to represent either direction.

$$\mu_i = p_i + eA_i \qquad (13)$$

Recalling Figure (1), the magnetic field B = ∇ x A is a constant (in the z-direction) so the canonical commutation relations can be described by Equation (14),

$$[x_i , p_j] = i\hbar\delta_{ij} \qquad (14)$$

which suggests that position and momentum do not commute, a key characteristic of all of quantum mechanics. We can use this fact along with the Hamiltonian structure of Equation (12) to derive ladder operators that will allow for the discovery of the allowed wave functions for this system.

$$a_{\pm} = \frac{1}{\sqrt{2e\hbar B}} (\mu_x \pm i\mu_y) \tag{15}$$

In Equation (15) a_+ denotes the "raising" operator and a_- the "lowing" operator, μ is defined as in Equation (13) above. This definition allows the Hamiltonian to be rewritten in terms of these new operators, shown in Equation (16) below.

$$H = \frac{\hbar eB}{m} (a_+ a_- + \frac{1}{2}) \tag{16}$$

Making use of Equation (14) along with the definitions for the raising and lowing operators a subsequent normalization leads to an identical definition as the one found for the case of the familiar simple harmonic oscillator. Shown by Equation (17) below, Ψ_n represents the wave function where n is the quantum number describing the particular state of that function.

$$a_+\Psi_n = \sqrt{n+1}\Psi_{n+1} \quad \text{and} \quad a_-\Psi_n = \sqrt{n}\Psi_{n-1} \tag{17}$$

With these new definitions, the time independent Schrodinger equation for this system can be solved by series method for its energy levels. I state the solution without further derivation as it simply presents a solution that is synonymous to that of the simple harmonic oscillation with a different angular frequency [18][19].

$$E_n = \hbar\omega_b(n + \tfrac{1}{2}) \tag{18}$$

In Equation (18) E represents the energy and ω_b represents the cyclotron frequency, $\omega_b = \frac{eB}{m}$, which describes the frequency of an electron in the presence of a constant magnetic field. This result is very important because it suggests that the energy levels of this system are equally spaced with a gap between them proportional to the magnetic field B. These are called the Landau levels [16][20].

1.3.1 Landau Gauge and Degeneracy

From Equation (12) it is clear that in order to find the wave functions for this system it is necessary to first define an appropriate gauge. I choose the Landau gauge as it is the easiest for rectangular geometries and it keeps the magnetic field invariant under both translational and rotational symmetry in the x-y plane. Another popular gauge is the symmetric gauge which I will not be using as it is slightly more complex and mainly useful for describing the fractional Hall effect, which is not the main focus of this paper [9][11][16]. With the magnetic field in the z-direction, B = ∇ x A, a value for the vector potential A can be selected for the Landau gauge,

$$A = xB\hat{j} \tag{19}$$

where in Equation (19) ĵ denotes the y-direction. This definition for A allows for the Hamiltonian to be rewritten as shown in Equation (20) below:

$$H = \frac{1}{2m}\left(p_x^2 + (p_y + eBx)^2\right) \tag{20}$$

As A, the magnetic vector potential, keeps its translational symmetry in the y-direction (ĵ) but not the x-direction there will be energy eigenstates that are also eigenstates of p_y. This suggests an ansatz solution for the wave function that depends on both an x and a y-component.

$$\Psi(x, y) = e^{iky} f_k(x) \tag{21}$$

In Equation (21) $\Psi(\mathrm{x}, \mathrm{y})$ represents the wave function ansatz solution, k is the wavenumber and $f_k(x)$ is the x-component function of the wave equation. Acting on this wave function with the Hamiltonian operator, Equation (20), will allow for the momentum, $p_{y,}$ operator to be replaced with ħk resulting in Equation (22).

$$\mathrm{H}\,\Psi(\mathrm{x}, \mathrm{y}) = H_k\,\Psi(\mathrm{x}, \mathrm{y}); \qquad H_k = \frac{1}{2m} p_x^2 + \frac{m\,\omega_b{}^2}{2}(\mathrm{x} + \mathrm{k}l_b^2)^2 \tag{22}$$

Here H_k is the Hamiltonian for a harmonic oscillator displaced from the origin by $\mathrm{k}l_b^2$ where l_b is the "magnetic length" defined as $l_b = \sqrt{\frac{\hbar}{eB}}$. This Hamiltonian form allows for a Hermite polynomial wave equation solution to be reached that depends on only two quantum numbers, n and k.

$$\Psi(\mathrm{x}, \mathrm{y})_{n,k} = e^{iky}(\mathrm{x} + \mathrm{k}l_b^2)e^{-(x+kl_b^2)^2/2l_b^2} \tag{23}$$

Equation (23), which presents the un-normalized solution, can be better visualized by looking at Figure (4) below with the e^{iky} component representing the momentum flux going into the page on the right and exiting on the left, as described by the cyclotron orbit [11][13][16].

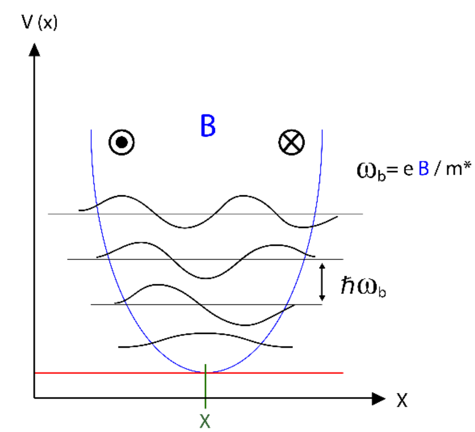

Figure 4: Theoretical plot of the landau levels and x-component wave functions of Equation (23). Here the slope of the potential is determined by the magnetic field, B. The energy levels are equally spaced as expected. X denotes the displacement from the origin, ω_b is the cyclotron freq. and m is the reduced mass of the electron [13].*

So far this Landau Quantization has been closely related to the physics of the simple harmonic oscillator (SHO), even deriving a similar energy spacing and wave function [18][19]. However, as Equation (23) depends on both n and k whereas the energy, Equation (18), depends on only n there is going to be a clear degeneracy per state that is drastically different than that of the SHO. For our rectangular sample of length, L (in the x-direction) and width, W (in the y-direction) we can restrict ourselves to this region and find out how many states will fit within this given area. Knowing the wave function is localized about $x = -kl_b^2$ where $0 \leq x \leq L$ it is clear that k will range between $\frac{-L}{l_b^2} \leq k \leq 0$, where the total number of states can be counted using Equation (24).

$$N = \frac{W}{2\pi}\int_{\frac{-L}{l_b^2}}^{0} dk = \frac{eBA}{2\pi\hbar} \tag{24}$$

In Equation (24), A is made to represent the area and N is the number of states within the sample. From this equation we are able to see that there will be a huge (but finite) number of degenerate states [11][12]. This number can be rewritten in terms of the magnetic flux contained within area $2\pi l_b^2$,

$$N = \frac{AB}{\Phi}; \qquad \Phi = \frac{2\pi\hbar}{e} \tag{25}$$

where in Equation (25) Φ is the quantum flux. This is especially important because the flux quantum per sample can be used to find out the total number of orthogonal eigenstates and will provide useful terminology for Section 2 [13].

2 The Quantum Hall Effect as a Topological State

The derivations and content presented in Section 1 of this paper should provide a sufficient description of the underlying physics of the quantum Hall effect, as well as some necessary background intuition as to why it can be described as a topological state. However, in order to successfully describe the quantum Hall effect topologically it is necessary to first present a more in depth look into how conductivity works in such a system. I begin with and will present most of this derivation in reference to the integer Hall effect as it ignores electron interactions and is therefore easier to illustrate making its topological nature much more transparent [2][21]. Additionally, focusing on the IQHE will allow for the definitions and equations presented in Section 1 to be referenced without having to drastically change them or provide a great deal of new information. With that being said, it is important to note that many of the general theoretical arguments made below, unless specifically specified, can be used to think about the FQHE topologically as well [9][11].

2.1 Integer Quantum Hall Effect

The integer Hall effect, first experimentally performed by von Klitzing in 1980, demonstrates a quantized Hall conductance, shown in Equation (1), with each transition occurring at integer values of η [2]. The results of this experiment are shown in Figure (3) with the top curve corresponding to the Hall resistance and the bottom curve corresponding to the longitudinal resistance [12]. As explained in Section 1.2 and 1.3 the experimental plots of Figure (3) drastically vary from those of the theoretical Drude model plots.

Due to the Landau-Fermi liquid theory, the integer Hall effect can be understood without considering electron interactions (besides Pauli exclusion principle), so the quantum states of a single particle described in Section 1.3 remain the same in a system containing many particles [11][21][22]. As each Landau level, denoted by quantum number η, can contain a large number of electrons, it is useful to define a filling factor to describe how the particles can occupy each level. The filling factor describes how many states are physically able to exist that are orthogonal to the original theorized wave function of Figure (4) within the given area of the two-dimensional sample. Orthogonal states will have separate orbits with an orbit center located at some distance away as defined by the magnetic length. In terms of the terminology provided by Equation (25), each orthogonal state can be said to be associated with the area of one flux quantum. This filling factor is seen in Equation (26) where ν is the filling factor, n_Φ is the degeneracy per unit area defined by Equation (25) (once divided by the area A), and n is the number of electrons in the sample [13].

$$\nu = \frac{n}{n_\Phi} \tag{26}$$

This value represents a filling factor that occurs per unit area of flux quantum and essentially quantizes how the Landau levels will be filled within the given area of the sample.

One of the most striking features of this result, as well as the data presented in Figure (3), is the fact that despite how the Landau levels are filled, the Hall resistivity seems to sit on a plateau for a range of magnetic field values instead of increasing linearly as one might expect from the more classical Drude model. This can be partially explained by making use of the convenient fact that the quantum number η corresponding to each Landau level is the same quantum number as defined in Equation (1) [9][11]. Relating these two like equations, the center of each plateau is seen to occur when the magnetic field takes on the value shown in Equation (27) below.

$$B = \frac{n}{\eta}\Phi , \qquad n = \frac{B\eta}{\Phi} \qquad (27)$$

Or in terms of n, the electron density, it appears that the density has to reach certain a value to get to each η^{th} plateau [13]. While this explanation helps to explain the filling of states required to reach each subsequent plateau it fails to explain the flatness of each plateau or how this effect can occur in a sample that is intrinsically dirty. Thankfully, these two stipulations, an unmistakable component of the quantum Hall effect, can be attributed to the effect's inherent topological nature [6][11][15].

2.2 Edge Modes

Thinking back to Equation (26) the filling of each Landau level occurs within some area of flux quantum. As the electrons fill each state, each orbiting around one area of flux quantum the filling factor, ν, increases. In this picture the electrons are able to complete their orbit without any other electron interactions or outside potential effecting their movement [13]. However, near the edges of the sample this area of orbit will be subject to a potential boundary which it cannot cross, and the motion of the electrons will be interrupted. These electrons, no longer able to complete a circular orbit, will instead interact with this boundary, striking the side and skipping along the potential barrier in a chiral motion; classically this is referred to as a skipping orbit [9][11][13].

A particle restricted to move in a single direction along a line is said to be chiral, this is important because something experiencing a chiral motion will have some very specific properties. In relation to condensed matter physics, the Nielsen-Ninomiya theorem demonstrates that you can't have charged chiral particles moving along a wire. You must also have particles which can move in the opposite direction as well [23]. Fortunately, the discussion and examples used in this thesis are able to somewhat side step this theorem as the chiral particles are seen to exist on the boundary of a two-dimensional system instead of on a one-dimensional wire. However, an important take away from the chiral nature of the edge modes besides the strictly singular direction of motion is the fact that there appears to be physical phenomena which can only take place on the boundary of a system [11].

Recalling the idea of skipping orbits, the edge barrier of the sample can be thought to cause a state of confinement, like that of an infinite well or box; the result being that the particles will be forced to move in one direction on one side of the sample, and in the other direction on the other side of the sample, ensuring that the net current, in the absence of an electric field will vanish. This property of the quantum Hall effect can be explained more quantitatively by simply modifying the Hamiltonian in Equation (20) with the addition of some potential V(x) as shown in Equation (28).

$$H = \frac{1}{2m}\left(p_x^2 + (p_y + eBx)^2\right) + V(x) \tag{28}$$

Here, as described above, the potential V(x) can be thought of as a hard wall potential barrier of effectively infinite height experienced by the sample boundary. Assuming the potential is smooth over distance scales of l_b we can Taylor expand the potential about some point x_o resulting in Equation (29).

$$V(x) \approx V(x_o) + (\frac{\partial V}{\partial x})(x - x_{o)} \dots \tag{29}$$

Dropping the constant term as well as any other quadratic terms Equation (29) shows that the wave function will experience a linear potential. This potential will in turn directly modify the allowed energy levels as seen in Equation (30) below [11][12].

$$E_{n,k} = ħω_b(n + \frac{1}{2}) + E(kl_b^2 - \frac{E}{mω_b^2}) + \frac{mE^2}{2B^2} \tag{30}$$

The addition to the energy equation, refencing Equating (18), makes sense conceptually as the orbit time for each electron, now interrupted by a barrier, will be essentially cut in half as they are no longer able to complete a full circular motion. Knowing that the frequency is inversely proportional to the energy, this effectively reduced orbit time should increase the energy as some function of k along the edges of the sample, a result we do see in Equation (30) [13].

The drift velocity of this system (in the y-direction) is defined by Equation (31) as:

$$v_y = \frac{1}{ħ}\frac{\partial E_{n,k}}{\partial k} = ħEl_b^2 = \frac{E}{eB} \tag{31}$$

Here as the electric field is related to the potential by E = -▽V this can be rewritten in relation to the linear edge barrier potential [8].

$$v_y = \frac{1}{eB}\frac{\partial V}{\partial x} \tag{32}$$

Equation (32) helps to show that the particles, drifting as a function of the barrier potential, will each have a wavefunction that sits at a different x-position with a different drift velocity. As expected from the more conceptual description of electron skipping orbits, the particles travelling along the edges will be chiral and opposite sides will travel contrary to one another [11].

Knowing that the edges of the sample carry electrons along in a chiral motion whereas the bulk of the material constricts electrons to some area of flux quantum allows for the conductivity of a sample experiencing the quantum Hall effect be better understood. For a specific value of B, with regards to the electron density, the bulk of the material will have filled states and therefore act as an insulator whereas the edge modes, filled with free electrons, will act like a metal [13]. To understand how the current works in this picture it is convenient to introduce some chemical potential Δμ that will fill up the conduction band with more states on one side than the other, shifting the Fermi energy [22]. This introduction of a chemical potential will populate free states and, due to more states being full on one side that the other, will create a current. With this addition from the chemical potential the current can be found by summing up these newly filled states.

$$I_y = -e \int \frac{dk}{2\pi} v_y(k) = \frac{e}{2\pi l_b^2} \int \; dx \frac{1}{eB} \frac{\partial V}{\partial x} = \frac{e}{2\pi\hbar} \Delta\mu \qquad (33)$$

In Equation (33) Δμ can be related to the Hall potential by $\Delta\mu = eV_H$ which by substitution will return the expected results of Equation (1) [11].

As suggested by looking at Figure (3), the conductivity of the quantum Hall effect will be flat with regards to the magnetic field, B, as each Landau level is filled. Knowing that the bulk of the material, which acts as an insulator, carries no current the current must therefore be carried entirely by the edge modes of the sample [6][11][15]. This fact, recalling from Section 1.2 that like trivial or non-trivial states can be transformed into one another, helps to define this property of the quantum Hall effect as topological. As the Landau levels are filled and electrons begin to occupy more and more states the conductivity will increase and jump up to each new plateau level. Every plateau can be defined as a different type of topological state which is entered by achieving a new ratio of magnetic field to carrier density.

2.3 Robust Quantum States

Another take away from Section 1.2 is the fact that, in terms of condensed matter physics, the topological character of states cannot change continuously [15]. While this is visibly apparent looking at the plateaued regions of Figure (3), this concept can be better understood by qualitatively defining the robustness of each Landau level. The scattering of electrons on the edge modes of the sample, as discussed above, has the unique property of being chiral in nature. This is important because electron scattering, which usually throws electrons in a random direction, will now only scatter the particles in the direction of the chiral motion. This means that the current carried by the sample along the edge modes is essentially immune to impurities. While this presents a nice relationship to describe the current, free from disorder, it is actually these impurities that exist within an inherently dirty sample that allow for the flat η valued plateaus, characteristic in the quantum Hall effect, to exist [11][13].

Considering the nature of the electrons near the Fermi surface there will be two quantum states allowed by this disorder, extended or localized. Here, an extended state is one that is spread throughout the whole system; these states will fall on a specific Landau level and will contribute to the conduction. In contrast, a localized state is one that is restricted to lie in some specific region of space. This state is caused by a potential “hills” or “valleys” trapping electrons and essentially forcing them to exist at a Fermi level that sits either above or below the Landau level [9][11][13][24]. This means that multiple localized states can be filled without effecting the conduction of the sample until a new Landau level is reached. This is the independence of the sample geometry hinted at in Section 1.1.1 and it is this phenomenon that can be held accountable for the robustness of each Landau level and distinguishable flatness of each plateau.

2.4 Chern Numbers

As a final motivation for the topological nature of the quantum Hall effect I present a short proof of the existence of integer states of the Hall conductivity, Equation (1), in terms of a topological invariant called a Chern number. This proof looks to demonstrate the topological nature of the IQHE by directly relating the quantum number η, from Equation (1), to the integer valued Chern number, C [25]. For this proof it is best to consider the effects of the IQHE constructed over a spatial torus. This shape is convenient because it allows for one to ignore the edge states. Additionally, if the wave function, Equation (23), were to be described using the Bloch theorem, which is not discussed in this paper, the resultant Bloch vector would be defined in a magnetic Brillouin zone which, in two dimensions, is topologically equivalent to a torus [6].

This setup can be effectively understood as a rectangle of side lengths L_x and L_y with opposite edges identified [6][11]. Sending a uniform magnetic field through the center of the torus we will want this field to abide by the Dirac quantization condition shown in Equation (34) below [11].

$$\mathrm{B}L_x L_y = \frac{2\pi\hbar}{e}\mathrm{n} \qquad (34)$$

As this torus will be subject to some magnet flux (locally perpendicular to the surface at every point), if the system is perturbed, it is important to consider the effects of this flux in terms of individual patches of area. This means that the wave functions must be related to one another via gauge transformation only.

This can be done by introducing a translational operator, T(d), which servers to translate a state, $\Psi(\mathrm{x},\mathrm{y})$, by a position vector d. In terms of this new operator, this system is further subject to the condition that when a state is translated around a cycle of the torus it must come back to itself, i.e. $T\ \Psi(\mathrm{x},\mathrm{y}) = \Psi(\mathrm{x},\mathrm{y})$ [6][11].

$$\mathrm{T(d)} = e^{-id\cdot p/\hbar} = e^{-id\cdot(i\nabla + eA/\hbar)} \tag{35}$$

From Equation (35) it is clear that the translational operator will depend on the definition for A, the magnetic vector potential. Recalling the Landau quantization from Section 1.3.1, I once again select the Landau gauge, Equation (19), as it keeps the magnetic field invariant under both translational and rotational symmetry along the x-y plane.

Applying this gauge to our translational operator, Equation (35), it appears that translation along the y-direction will pick up an extra phase not seen in the x-direction. This is demonstrated in Equations (36) and (37).

$$T_x\ \Psi(\mathrm{x},\mathrm{y}) = \Psi(\mathrm{x} + L_x,\ \mathrm{y}) \tag{36}$$

$$T_y\ \Psi(\mathrm{x},\mathrm{y}) = e^{ieBL_y x/\hbar}\Psi\left(\mathrm{x},\ \mathrm{y} + L_y\right) \tag{37}$$

From these equations it is apparent that the wave functions will only agree up to a gauge transformation as they are inconsistent for all choices of B [11]. If we apply the translational operator in either the x, then the y-direction or vice versa we will arrive at the relationship shown in Equation (38) below.

$$T_x T_y = e^{ieBL_y L_x/\hbar} T_y T_x \tag{38}$$

This is especially revealing as it returns us to the Dirac quantization conditions, put forward in Equation (34) [11].

In order to see how the flux, the whole reason for the translational operator, acts upon the torus we must perturb the system. This can be done by modify the Landau gauge with the addition of some flux Φ_i where i refers to either the x or the y-direction as seen in Equations (39) and (40).

$$A_x = \frac{\Phi_x}{L_x} \tag{39}$$

$$A_y = \frac{\Phi_y}{L_y} + Bx \tag{40}$$

Here it is important to note that if Φ_i is increased from 0 to Φ, Φ being the quantum flux presented in Equation (25), the spectrum of the quantum system will be invariant as the states are only sensitive to the non-integer parts of $\frac{\Phi_i}{\Phi}$ [6][9][11][13].

The addition of flux to this system will modify the Hamiltonian by some factor

H = H_o + ΔH where H_o represents the Hamiltonian of an unperturbed system and ΔH accounts for the added flux [26].

$$\Delta H = -J \cdot A = \sum_{i=x,y} \frac{J_i \Phi_i}{L_i} \tag{41}$$

In Equation (41) J is the current density and A is the magnetic vector potential. We can use this new Hamiltonian to see how the ground state of this system will be affected by the presence of the added flux perturbations. Assuming the ground state is non-degenerate and separated from the first excited state by some energy gap, $\hbar\omega_b$, we can modify our original ground state wave function.

$$|\Psi_o\rangle' = |\Psi_o\rangle + \sum_{n\neq\Psi_o} \frac{\langle n|\Delta H|\Psi_o\rangle}{E_n - E_o}|n\rangle \tag{42}$$

Here in Equation (42) Ψ_o represents the ground state wave function and Ψ_o' is the modified wave function, Bra-Ket notation is used for the sake of convenience. As we chose to think of the flux through this system in terms of small patches of area, we are going to want to consider the infinitesimal changes to Φ_i which are shown by Equation (43) below.

$$|\frac{\partial\Psi_o}{\partial\Phi_i}\rangle = -\frac{1}{L_i}\sum_{n\neq\Psi_o} \frac{\langle n|J_i|\Psi_o\rangle}{E_n - E_o}|n\rangle \tag{43}$$

Equation (43) looks incredibly familiar to the Kubo formula for the Hall conductivity describing the general, multi-particle Hamiltonian H_o. The Kubo formula is most commonly used to expresses the linear response of an observable quantity due to a time dependent perturbation and is often applied to describe electron systems similar to that of this discussion. This solution, which serves to define the conductivity in terms of the individual contribution from each energy level, is stated without derivation below [11][26].

$$\sigma_{xy} = i\hbar L_x L_y \sum_{n\neq\Psi_o} \frac{\langle\Psi_o|J_y|n\rangle\langle n|J_x|\Psi_o\rangle - \langle\Psi_o|J_x|n\rangle\langle n|J_y|\Psi_o\rangle}{(E_n - E_o)^2} \tag{44}$$

In Equation (44) σ_{xy} represents the Hall conductance with directional components referencing the conductivity tensor previously defined by Equation (7).

Using this formula along with the correct factors for the spatial area of the torus allows for the conductivity to be rewritten in terms of Equations (42) and (43).

$$\sigma_{xy} = i\hbar \left[\langle\frac{\partial\Psi_o}{\partial\Phi_y}|\frac{\partial\Psi_o}{\partial\Phi_x}\rangle - \langle\frac{\partial\Psi_o}{\partial\Phi_x}|\frac{\partial\Psi_o}{\partial\Phi_y}\rangle\right]$$

$$= i\hbar \left[\frac{\partial}{\partial\Phi_y}\langle\Psi_o|\frac{\partial\Psi_o}{\partial\Phi_x}\rangle - \frac{\partial}{\partial\Phi_x}\langle\Psi_o|\frac{\partial\Psi_o}{\partial\Phi_x}\rangle\right] \tag{45}$$

In Equation (45) the conductivity is written in such a way that the fluxes, Φ_i can be seen to parameterize the perturbed Hamiltonian [6][11].

2.4.1 Berry Phase

Before completing this proof, we require a brief introduction to the concept of the Berry phase. For a quantum system in a certain eigenstate, an adiabatic evolution of the Hamiltonian will show system to remain in that same eigenstate of the Hamiltonian, while now obtaining a phase factor. This factor is called the Berry phase [27].

$$|\Psi\rangle \rightarrow e^{i\gamma}|\Psi\rangle \quad (46)$$

In Equation (46) $e^{i\gamma}$ describes the phase obtained after adiabatic evolution. Knowing that this phase is related only to the adiabatic evolution as it leaves and returns to its original state it will have a certain time independence described by Equation (47) below.

$$U^*\dot{U} = -\langle n|\dot{n}\rangle = -\langle n|\frac{\partial}{\partial\lambda^i}|n\rangle\,\dot{\lambda}^i \quad (47)$$

In Equation (47) U represents some time dependent phase that defines the phase of the wave function in terms of some reference state (much like that of the Berry phase); n is the eigenvalue corresponding to the particular state of the wavefunction, and $\lambda(t)$ is simply used to parameterize the Hamiltonian as a function of time. This definition can be simplified by the formation of something called the Berry connection.

$$A_i(\lambda) = -i\langle n|\frac{\partial}{\partial\lambda^i}|n\rangle \quad (48)$$

This connection, shown in Equation (48), is very useful because it can essentially be treated as a gauge potential such that,

$$A_\mu \rightarrow A_\mu' = A_\mu + \partial_\mu f(x) \tag{49}$$

for any function of f(x). In Equation (49) μ = 0, 1, 2… which represents coordinates in Minkowski spacetime and A_μ' represents the new potential after transformation. This definition allows us to compute the field strength as given in Equation (50) below.

$$F_{\mu\nu} = \frac{\partial A_\mu}{\partial x^\nu} - \frac{\partial A_\nu}{\partial x^\mu} \tag{50}$$

Here Equation (50) reflects the force contribution of both the electric and magnetic fields and has the important quality of being invariant under gauge transformation [6][8][11][27].

Now equipped with this useful information about the Berry phase, we can return to the spatial torus proof from before. Recalling from Equation (45) the fluxes, Φ_i, are seen to parametrize the perturbed Hamiltonian. As the spectrum of this Hamiltonian depended on only Φ_i and Φ it is convenient to define a new dimensionless variable to simplify things.

$$\theta_i = \frac{2\pi\Phi_i}{\Phi} \tag{51}$$

In Equation (51) theta must be contained between 0 and 2π as it is being used to parametrize the circular torus. Given this new parameter space we can now consider the Berry phase that exists if this parameter is varied. Applying the more general definition for the Berry connection, Equation (48), to the torus will result in Equation (52),

$$A_i(\Phi) = -i\langle\Psi_o|\frac{\partial}{\partial\theta^i}|\Psi_o\rangle \tag{52}$$

allowing us to once again define the field strength, Equation (50) in terms of this new Berry connection.

$$F_{xy} = \frac{\partial A_x}{\partial \theta_y} - \frac{\partial A_y}{\partial \theta_x} = \mathrm{i}\left[\frac{\partial}{\partial \theta_y}\langle \Psi_o | \frac{\partial \Psi_o}{\partial \theta_x}\rangle - \frac{\partial}{\partial \theta_x}\langle \Psi_o | \frac{\partial \Psi_o}{\partial \theta_x}\rangle\right] \tag{53}$$

Looking back at the conductivity, Equation (45), it is clear that Equation (53) presents the same exact result minus a constant factor. This fact allows us to redefine the conductivity for our torus system, now experiencing flux, in terms of the field strengths [6][11][27].

$$\sigma_{xy} = -\frac{e^2}{\hbar} F_{xy} \tag{54}$$

This might look finished, however, we are not quite done as Equation (54) does not account for the whole picture. Recalling that we originally considered the flux in small patches of area, in order to correctly quantize the conductivity, σ_{xy}, we need to sum up the total flux contribution over the entire torus.

$$\sigma_{xy} = -\frac{e^2}{\hbar} \int \frac{d^2\theta}{(2\pi)^2} F_{xy} \tag{55}$$

In Equation (55) this integral over the curvature of the torus can be redefined to instead refer to the quantization of the conductivity in terms of the first Chern number [11].

$$\mathrm{C} = \frac{1}{2\pi} \int d^2\theta \, F_{xy} \tag{56}$$

Where in Equation (56) C is a Chern number which always has an integer value [25]. This average over all the flux contributions in terms of Chern numbers ultimately results in the same quantization as that of the Hall conductivity seen in Equation (1).

$$\sigma_{xy} = \frac{e^2}{2\pi\hbar} C \tag{57}$$

The result presented in Equation (57) helps to make a very strong argument for the topological nature of the quantum Hall effect as Chern numbers are considered to be topological invariants. It is important to note that as Chern numbers are always integer this derivation, while insightful, only applies to the IQHE [6][11].

3 Conclusion

The study of topological quantum matter was pioneered with the discovery of the integer, and later fractional quantum Hall effects in the two-dimensional electron systems of semiconductor devices. These effects demonstrated, through a number of unique and at the time unexpected properties, that quantum states of matter could be described using topology [6]. Relying on several increasingly more complex "toy models" the topological nature of the quantum Hall effect can be demonstrated by looking at the conductivity, energy levels, and gauge invariant properties of electrons confined to a two-dimensional material under the presence of a strong magnetic field.

As described in Section 2 the properties exhibited by the electrons reveal that they are in the QHE state. These electrons, due to the nature of quantum entanglement, experience some unusual characteristics near the edges of a material where the entanglement stops. Here the current is seen to be carried entirely by the edges modes as the charged particles slide along the edges of a sample in a chiral motion, regardless of its geometry or inherent dirtiness [9][11][13].

Looking at the overall conduction of the quantum Hall effect we saw that the inherent impurities within the sample could be attributed to the overall robustness of the effects quantum states. As electrons are able to fill both extended and localized states this robust property does not show a linear resistivity, instead quantizing the conductivity as it jumped up from one conduction level to another. Knowing that topologically defined states cannot change continuously from Section 1.2, this property of the effect further helped to link the ideas of topology to quantum states of condensed matter defining each new plateau as a different type of topological state. [11][13][15].

Finally, the topological properties of the quantum Hall effect were further investigated by looking at the specific case of the IQHE constructed over a spatial torus. This proof served to relate Chern numbers, a topological invariant, to the known quantized conductivity presented in Equation (1) demonstrating the clear connection between topology and quantum states of matter [6][9][11][25].

Overall the quantum Hall effect's unique properties could be used to better understand electron-electron interactions in two dimensions by describing certain aspects of the effect topologically. The impact of topology within this subject and even the broader field of condensed matter physics was demonstrated by detailing several key characteristics of this effect.

3.1 Modern Applications of the Quantum Hall Effect

Quantum Hall physics, or the study of the quantum Hall effects is an ever-growing subsect of condensed matter physics that does not end with the simple explanations I provided. Current research looks to further identify more fractional values of η as well as observe these effects in other two-dimensional material such as graphene [28]. One of the more compelling future applications of this effect has to do with the discovery of certain fractional values in the

FQHE that resulted in elementary excitations called anyons [9][11]. These anyons are seen to have fractional statistics that correspond to neither fermions or bosons and may play an important role in the future of topological quantum computation. The quantum Hall effect also greatly contributes to other related fields of study including the subjects of topological insulators and topological order.

Generally, the interest in quantum Hall physics stems from its relation to both low dimensional quantum systems and systems with strong electronic correlations [11]. Discovery of the quantum Hall effect as a topological quantum system also resulted in the Nobel prizes for the experimental verification of the IQHE by von Klitzing in1985 and for the FQHE by Stormer, Tsui and Laughlin in 1998. This effect even played a major role in the research behind the 2016 Nobel prize which was rewarded for theoretical discoveries of topological phase transitions and topological phases of matter [9][6].

4 Acknowledgements

I would especially like to thank Professor Ramirez for his advice and help with this thesis.

5 Bibliography

[1] Ando, Tsuneya; Matsumoto, Yukio; Uemura, Yasutada (1975); Theory of Hall Effect in a Two-Dimensional Electron System; Journal of the Physical Society of Japan, Volume 39, Issue 2, pp. 279-288;

[2] Klaus von Klitzing (1980); New Method for High-Accuracy Determination of the Fine-Structure Constant Based on Quantized Hall Resistance; Rev. Mod. Phys. Volume 45, Number 6; 11 August 1980; pp. 494-497;

[3] Tsui, D. C.; Stormer, H. L.; Gossard, A. C. (1982); Two-Dimensional Magneto-transport in the Extreme Quantum Limit; Physical Review Letters, Volume 48, Issue 22, May 31, 1982, pp. 1559-1562;

[4] Willett; Eisenstein; Stormer et al. (1987); Observation of an Even-Denominator Quantum Number in the Fractional Quantum Hall Effect; Rev. Mod. Phys. Volume 59, Number 15; 12 October 1987; pp. 1776-1779;

[5] R. B. Laughlin (1983); Anomalous Quantum Hall Effect: An Incompressible Quantum Fluid with Fractionally Charged Excitations; Rev. Mod. Phys. Volume 50, Number 18; 02 May 1983; pp. 1395-1398;

[6] F. Duncan; M. Haldane (2017); Nobel Lecture: Topological quantum matter; Rev. Mod. Phys. Volume 89, Number 4; pp. 1-10;

[7] Hall, E. H. (1879); On a New Action of the Magnet on Electric Currents; American Journal of Mathematics, 2, No. 3, pages 287–292;

[8] Griffiths, David J. *Introduction to Electrodynamics*. Fourth ed. Cambridge University Press, 2017. Print, pp 78-79, 256-257, 562-570.

[9] Goerbig, M. O. (2009); Quantum Hall Effect; arXiv:0909.1998v2; Digital Print.

[10] Weiss D. (1995) Transport in Antidot Superlattices. In: Cerdeira H.A., Kramer B., Schön G. (eds) Quantum Dynamics of Submicron Structures. NATO ASI Series (Series E: Applied Sciences), vol 291. Springer, Dordrecht.

[11] Tong, David (2016); Lectures on the Quantum Hall Effect, arXiv:1606.06687v2; Digital Print.

[12] Klitzing, Klaus (1986); The Quantized Hall Effect, Rev. Mod. Phys. Volume 58, Issue 3, July 1986, pp. 519-531;

[13] Grayson, Matthew (2015); Northwestern University; TAUVOD. “Integer and Fractional Quantum Hall Effects: An Introduction.” Video Lecture.

[14] Kelly, John L. *General Topology*. First ed. Mineola: Dover Publications, Inc., 2017. Print.

[15] Haldane, Duncan (2017); Princeton University; Apsphysics. “Topological States of Quantum Condensed Matter: Duncan Haldane.” Video Lecture.

[16] Murayama, Hitoshi (2014); Lectures on Landau Quantization and Levels, The University Berkeley of Berkeley Library; Digital Print.

[17] Taylor, John R. *Classical Mechanics*. First ed. University Science Books, 2005. Print, pp 522-538.

[18] Harris, Randy. *Modern Physics*. Second ed. Davis: Jim Smith, 2008. Print, pp 164-169.

[19] Griffiths, David J. *Introduction to Quantum Mechanics*. Second ed. Cambridge University Press, 2017. Print, pp 40-57.

[20] Hurd, Colin M. (1972), The Hall Effect in Metals and Alloys, Plenum Press, New York.

[21] L. D. Landau (1956); The Theory of a Fermi Liquid; Physical Review Letters, Volume 3, Issue 6, March 7, 1956, pp. 920-925;

[22] Simon, Steven H. *The Oxford Solid State Basics*. First ed. Oxford University Press, 2013. Print, pp 28-38, 173-190.

[23] H. B. Nielsen, M. Ninomiya (1981); A no-go Theorem for Regularizing Chiral Fermions; Physical Review Letters, Volume 105, Issue 2, 1981, pp. 219-223;

[24] Ando, Tsuneya; (1983); Electron Localization in a Two-Dimensional System in Strong Magnetic Fields; Journal of the Physical Society of Japan, Volume 52, pp. 1740-1749;

[25] Takahiro Fukui, Yasuhiro Hatsugai, Hiroshi Suzuki (2005); Chern Numbers in Discretized Brillouin Zone: Efficient Method of Computing (Spin) Hall Conductances; Journal of the Physical Society of Japan, Volume 74, pp. 1674-1677;

[26] Crepieux, A., Bruno, P; (2001); Theory of the anomalous Hall effect from the Kubo formula and the Dirac equation; Phys. Rev. B64, 014416;

[27] Di Xiao, Ming-Che Chang, Qian Niu; (2010); Berry phase effects on electronic properties; Rev. Mod. Phys. 82, 1959;

[28] Moon, Pilkyung; Koshino, Mikito (2012); Energy spectrum and quantum Hall effect in twisted bilayer graphene; Rev. Mod. Phys. B 85; 29 May 2012; pp. 1-9;